

Density of states of disordered systems

M. C. W. van Rossum and Th. M. Nieuwenhuizen

van der Waals-Zeeman Laboratorium, Universiteit van Amsterdam, Valckenierstraat 65, 1018 XE Amsterdam, The Netherlands

E. Hofstetter and M. Schreiber

Institut für Physikalische Chemie, Johannes-Gutenberg-Universität, Jakob-Welder-Weg 11, 55099 Mainz, Federal Republic of Germany

(Received 1 November 1993)

Density of states calculations for the tight-binding model with diagonal disorder are presented. An instanton approach is used to calculate the tails of the spectrum, including all prefactors. It is shown that a Hartree resummation improves the predictions. Furthermore, an effective-medium approximation is used to calculate the density of states in the band. Combining both approaches, a prediction is obtained for all energies. Large numerical simulations have been performed to check the validity of the approach for the Anderson model with Gaussian and with binary disorder on square and simple cubic lattices. The theory agrees well with the simulations.

I. INTRODUCTION

In pure crystalline solids, electronic excitations have a band structure. Energy intervals in which excitations occur are separated by band gaps, where the density of electronic states vanishes. At the band edges the density of states has power law singularities, so-called van Hove singularities. When a random potential is present, the situation changes. States occur inside the band gaps of the unperturbed system. This has two effects. First, the band broadens as the band edges shift. Second, the singularities of the density of states smear out: the density of states will have tails. The randomness can have various origins. The model could for instance be used to describe binary alloys; the random potential has a binary distribution. The model can also represent independent electrons interacting with lattice vibrations in a pure crystal. In this case the disorder is caused by displacement of atoms. On short time scales the disorder is static and has a Gaussian distribution.¹ Urbach noticed that his experiments on the latter type of system could roughly be described by an exponential tail, the Urbach tail.² Urbach originally stated his experimental rule for the absorption intensity, which is closely related to the density of states. Theoretical results for the tails of the density of states are available for binary disorder (Lifshitz tail³), for Gaussian disorder in continuous and discrete space (Halperin-Lax tail^{4,5}), and for the Lloyd model.⁶

The problem of the density of states of disordered systems has been studied extensively and is of practical importance (see Ref. 7 for a recent review). Most of the approaches fall into two categories. One way is to use diagrammatic expansions like the *coherent-potential approximation* (CPA) or related methods.^{1,8,9} The CPA has been checked for various systems against numerical

work.¹⁰ The CPA works well if the values of the random potential are not bounded, as in the case of Gaussian disorder. However, the CPA fails to predict the tail of the density of states if the random values of the potential are bounded, as in the case of binary disorder. Another way is to perform an exact average of the randomness, which results in a field theory with an effective interaction stemming from the disorder. The density of states in the tail is determined by an instanton solution of this theory. This general approach has also been used for spatially correlated disorder.¹¹ However, the determination of the prefactors has only been done a few times. It was done analytically in special cases only.¹³⁻¹⁵ Recently a more general approximation was made, but renormalization, which we show to be important, was not performed.¹² In one-dimensional systems the analysis of exact integral equations has led to additional results for binary disorder, exponential disorder, and arbitrary disorder (see Ref. 16 and references therein).

It is the purpose of the present work to provide a more general theory for the tail of the density of states without adjustable parameters. We have also performed extensive numerical simulations, which extend previous results¹⁷ to more and larger systems. Thus the statistical fluctuations, even in the far tail, are small, and a comparison with the theoretical predictions over a large energy range can be made. The instanton approach is introduced in the next section, and its fluctuations are discussed in Sec. III. In Sec. IV we show that Hartree resummation improves our results. Furthermore, we present in Sec. V an effective-medium theory to calculate the density of states in the rest of the spectrum. The numerical method is discussed in Sec. VI; the data are compared with theory in Sec. VII. The paper closes with a summary. Some simple cases were already treated earlier.¹⁸

II. INSTANTON APPROACH

Consider the Anderson model with static diagonal disorder on a hypercubic lattice with unit lattice constant. Hopping is described by a lattice Laplacian. The potential V is random. At each lattice site, its value is independently drawn at random from a distribution $\nu(V)$. The Hamiltonian is thus given by

$$H = -\Delta + V. \quad (1)$$

The density of states is defined as

$$\rho(E) = \lim_{N \rightarrow \infty} \frac{1}{N} \sum_{i=1}^N \delta(E - E_i), \quad (2)$$

where N is the number of lattice points and where the E_i are the eigenvalues of the Schrödinger equation. As the density of states is self-averaging, the large- N limit yields the average density of states. The average density of states can be extracted from the Green's function, $G = (H - E)^{-1}$, as

$$\rho(E) = \frac{1}{\pi N} \sum_r \text{Im Tr } \langle G(E + i0) \rangle_{r,r}. \quad (3)$$

The angular brackets indicate averaging over the disorder configurations. This average can be taken either by using the replica trick, or by introducing a supersymmetric field.¹⁹ We use the latter procedure. The Green's function is written as a path integral,

$$G_{r,r'}(E) = \int D\bar{\Psi} D\Psi \exp \left[\sum_r -\bar{\Psi}_r (-\Delta - E + V_r) \Psi_r \right] \times \phi_r^* \phi_{r'}. \quad (4)$$

This involves the two-component field $\Psi_r = (\phi_r, \chi_r)$, where ϕ_r is a boson field and where χ_r is a Grassmann field.^{19,20} The field ϕ_r takes values on the line $(-\infty\sqrt{i}, +\infty\sqrt{i})$. Due to the combination of fields the normalization of the Green's function has canceled in this expression. This allows the Green's function to be averaged over the impurity potentials, yielding

$$\langle G(E) \rangle_{r,r'} = \int D\bar{\Psi} D\Psi \exp(-A) \phi_r^* \phi_{r'}, \quad (5)$$

with an action

$$A = \sum_r [-\bar{\Psi}_r (\Delta \Psi)_r - E \bar{\Psi}_r \Psi_r + U(\bar{\Psi}_r \Psi_r)]. \quad (6)$$

The effective potential U follows from the distribution of the disordered potentials $\nu(V)$,

$$U(x) = -\ln \int_{-\infty}^{\infty} dV \nu(V) e^{-Vx}. \quad (7)$$

Formulas (3)–(7) can be used on a lattice or in the continuum, regardless of the disorder distribution or dimension. For Gaussian disorder with zero mean and variance $\langle V_r^2 \rangle = \sigma^2$, one finds $U(x) = -\sigma^2 x^2 / 2$. This leads

to a field theory with a ϕ^4 interaction. For the case of binary disorder with zero mean, we assume that the potential has a probability c that $V_r = (1 - c)V_0$ and a probability $1 - c$ that $V_r = -cV_0$. One then finds $U(x) = -\ln(1 - c + ce^{-V_0 x}) - cV_0 x$. In a binary alloy c corresponds to the concentration of one of the species.

Under general conditions the resulting nonlinear field equations have saddle point solutions (also called classical solutions or instantons).²¹ In the tail of the density of states this solution is dominant. For reasons of convenience we will only consider the low-energy tail of the lowest energy band. The action is minimal if the center of mass of the instanton is exactly located on a lattice site. The action is stationary when the equation of motion is satisfied. The solution f has to satisfy

$$-\Delta f - Ef + U'(f^2)f = 0. \quad (8)$$

The solution with the lowest action is selected from all possible solutions, as the other instantons give negligible contributions to the density of states. The action of this instanton is denoted as A_c and can be expressed as

$$A_c = \sum_r U(f_r^2) - f_r^2 U'(f_r^2). \quad (9)$$

Inserting A_c for A in Eq. (5) gives the exponent of the density of states (3). This exponent of the density of states has already been studied in the literature for some cases; see, for instance, Ref. 20.

The saddle point solutions are degenerate in several ways. We lift one degeneracy by fixing the instanton in the boson direction, and insert $\Psi_r = (f_r, 0)$. We also fix the center of the instanton inside the unit cell containing the origin of the lattice. This choice is also arbitrary and yields a factor N , which cancels the factor $1/N$ in the expression for the density of states (2).

III. FLUCTUATIONS AND THE PREFACTOR OF THE DENSITY OF STATES

Important here is the treatment of the prefactor of the density of states. It is determined by the fluctuations around the instanton. We thus put $\Psi_r = (f_r, 0) + (\delta\phi_r, \delta\chi_r)$. We approximate most of the fluctuations by their quadratic terms, leading to determinants of the fluctuation matrices. If this were done for all fluctuations one would find

$$\begin{aligned} \langle G_{r,r}(E) \rangle &= \int D\bar{\Psi} D\Psi \exp(-A_c + \delta\chi^* M_T \delta\chi \\ &\quad + \delta\phi^* M_L \delta\phi) f_r^2 \\ &= e^{-A_c} \sqrt{\frac{\det M_T}{\det M_L}} \sum_r f_r^2. \end{aligned} \quad (10)$$

This expression involves the determinants of the longitudinal and transversal fluctuation matrices,

$$\begin{aligned} M_L &= -\Delta - E + U'(f^2) + 2f^2 U''(f^2), \\ M_T &= -\Delta - E + U'(f^2). \end{aligned} \quad (11)$$

The determinants can be calculated analytically for some cases. An example is the white-noise potential on a line.¹⁵ In general they have to be determined numerically. However, as is well known, *zero modes* and *nearly zero modes* are also present, and have to be treated separately. The integration over the zero-mode fluctuations can be done by a change of variables to collective coordinates.²² Both in the continuum and on the lattice the matrix M_T has one zero eigenvalue, corresponding to supersymmetric rotation. (Or rotation in replica space if the replica trick is used to average the Green's function.) This eigenvalue has to be excluded from the evaluation of the determinant; instead a factor $\sqrt{\pi/\sum_r f_r^2}$ will enter in Eq. (10). This involves the norm $(\sum_r f_r^2)^{1/2}$ and a factor $\sqrt{\pi}$, compensating the omission of the eigenvalue in the determinant.

The behavior of the longitudinal matrix is more subtle. In the continuum, due to translational invariance, M_L will have d zero modes. These generate a shift of the instanton. Their eigenvalues should also be excluded from the determinant. Their resulting factor is $[\sum_r (\frac{\partial f}{\partial x})^2 / \pi]^{d/2}$. We return to the situation on the lattice. In the case of Gaussian disorder only the zero mode of M_T remains. The zero modes of M_L disappear, expressing the fact that the Gaussian instanton is strongly bound to the lattice. An instanton with its center a little bit shifted has a much larger action and barely contributes to the path integral. All M_L fluctuations can be approximated quadratically. Thus the density of states in the tail for Gaussian disorder is

$$\rho(E) = \left(-\frac{\det' M_T \sum_r f_r^2}{\det M_L \pi} \right)^{1/2} \exp(-A_c). \quad (12)$$

The prime indicates here the exclusion of the zero mode.

In the case of binary disorder the situation is more complicated as we are dealing with a crossover regime between the quadratic approximation and real zero modes. On the lattice, nearly zero modes of M_L are present; they are the remainders of the translational zero modes of M_L in the continuum. This means that the action varies only slightly (essentially quartically) under such variations. Large fluctuations, shifting the center of the instanton, give an important contribution to the action. Even an instanton shifted to the edge of the unit cell gives a significant contribution. It is not allowed to shift the instanton outside the unit cell, as instantons centered inside other unit cells are already taken into account. This makes an analytical treatment difficult. We therefore integrated numerically over these fluctuations. The integration boundaries are chosen such that the fluctuations do not shift the center of the instanton outside the unit cell. Let g_r^i , $i = 1, \dots, d$ denote the (normalized) nearly zero modes. The integral over the fluctuations of these modes now is

$$K = \int dc^1 \dots dc^d \exp[-A(f + c^i g^i) + A_c] \times \xi \left(\frac{\sum_r r(f_r + c^i g_r^i)}{\sum_r (f_r + c^i g_r^i)} \right), \quad (13)$$

in which sums over i are implied. $\xi(r)$ is the characteristic function of the unit cell. [$\xi(r) = 1$ if r is inside the unit cell containing the origin, else $\xi(r) = 0$.] This factor fixes the integration boundaries. Having integrated explicitly over these fluctuations, the small eigenvalues corresponding to these modes are to be excluded from the determinant. Integrating over all fluctuations one finally obtains for the density of states in the tail for binary disorder:

$$\rho(E) = K \left(-\frac{\det' M_T \sum_r f_r^2}{\det' M_L \pi} \right)^{1/2} \pi^{d/2} \exp(-A_c). \quad (14)$$

The primes now indicate the exclusion of the exactly zero mode in the M_T determinant, and the d nearly zero modes in the M_L determinant. Note that this expression is general: it also contains the case of Gaussian disorder, where K can be evaluated analytically.

The above "bare" results yield the density of states for energies between the minimal value of the random potential and zero. Equation (14) correctly describes the far tail, yet it diverges from the numerical data when approaching the band edge.

IV. HARTREE RESUMMATION

The above theory can be improved by performing a loop renormalization or Hartree resummation.^{15,23} In the continuum, renormalization is needed in two or more dimensions to obtain a finite density of states.¹⁴ Although on the lattice the result without renormalization is finite, renormalization improves the prediction for the density of states. In the case of Gaussian disorder, we are dealing with a ϕ^4 interaction. Resummation of the interaction term shifts the effective energy to a renormalized energy E_R . Some additional improvement can be made by doing the resummation self-consistently:

$$E_R = E + \sigma^2 g_0(E_R), \quad (15)$$

with g_0 being the return Green's function,

$$g_0(E) = \int_{-\pi}^{\pi} \frac{d^d q}{(2\pi)^d} \frac{1}{-\Delta(q) - E}, \quad (16)$$

in which $\Delta(q)$ is the momentum representation of the Laplacian. In the case of binary disorder, the interaction can be expanded in ϕ^{2n+2} terms. Similar loop corrections are made in all these interaction terms. The resummation leads to an effective potential for the binary case given by¹⁵

$$U_R(x, g_0) = -cV_0 x - \sum_{m=1}^{\infty} \frac{1}{m} \left(\frac{-c}{1-c} \right)^m \times \left[1 - \exp \left(\frac{-mxV_0}{1 + mg_0(E_R)V_0} \right) \right]. \quad (17)$$

We use the renormalized potential to refine the prediction for the density of states. We write $U = U_R + (U - U_R)$ and we treat $(U - U_R)$ as a perturbation. The instanton

and the fluctuation matrices are recalculated with the renormalized energy and potential. The change in the potential is compensated afterwards,

$$\rho_R(E; U) = \rho(E, U_R) e^{\sum_r [U_R(f^2) - U(f^2)]}. \quad (18)$$

$\rho(E, U_R)$ is calculated as in Sec. III, but with the resummed potential.

The energy range where the instanton contribution is dominant is smaller than in the bare case. The limiting energy shifts away from the band center. Comparison with numerical simulation will show that resummation significantly improves the prediction for the density of states.

V. EFFECTIVE-MEDIUM THEORY

We also present an effective-medium theory for the density of states inside the band. As stated above, the tail of the density of states is dominated by the instanton solution of field equation (6). Nearer to the band center, however, the trivial solution ($f = 0$) is the most important. The same resummation as in the tail is made, but now only the self-energy correction is taken into account. Interaction terms remaining after resummation are neglected. We obtain a self-consistent equation for the return Green's function g_0 ,

$$g_0 = \left(\frac{1}{-\Delta - E + U'_R(0, g_0)} \right)_{0,0}, \quad (19)$$

in which $U'_R(0, g_0) = \left. \frac{dU_R(x, g_0)}{dx} \right|_{x=0}$. Since g_0 is a complex quantity now, the density of states can be extracted immediately, using

$$\rho(E) = \frac{1}{\pi} \text{Im } g_0(E + i0). \quad (20)$$

Although this may not be the best theory for the density of states in the band center (CPA, for instance, is better in the cases considered), it has a nice feature: It precisely complements the instanton prediction for the density of states (12) and (14). The transition between the renormalized instanton and this regime occurs at the band edge of the effective-medium theory. This band edge is given by

$$\frac{dE}{dE_R} = 0, \quad (21)$$

with

$$E = E_R + U'_R(0, g_0), \quad (22)$$

involving $g_0(E_R)$ from Eq. (19).

We stress that the behavior found in this region is unphysical. It was not the goal of this study to resolve this; however, we expect the discrepancies to disappear when the critical region is dealt with properly.

VI. NUMERICAL SIMULATION

To corroborate the validity of the theory presented and in particular to evaluate the improvement by resummation, we have performed extensive numerical simulations. In site representation the Anderson Hamiltonian (1) can be expressed as

$$H = \sum'_{i,j} |i\rangle t \langle j| + \sum_j |j\rangle V_j \langle j|, \quad (23)$$

where the primed sum involves summation over nearest-neighbor pairs. We choose the transfer matrix element $t = 1/\nu$ (where ν is the number of nearest neighbors) so that the band extends between -1 and 1 for $V_j = 0$.

In numerical investigations of the Anderson model, the disordered potentials V_j have usually been chosen according to a box distribution of width W/t , i.e., a variance $\sigma^2 = W^2/12$. For the present comparison we have used the Gaussian and the binary distributions. We note for completeness that we shifted the mean of either distribution to νt , so that the band edge of the system without disorder appears at $E = 0$, in agreement with the representation (1) of this model.

As the secular matrix corresponding to the Hamiltonian (23) is extremely sparse (five or seven nonvanishing elements in each row and column in two or three dimensions, respectively), and as we are interested in the eigenstates at extreme energies, the straightforward diagonalization of the secular matrix can be most effectively performed by the Lanczos method. We used this algorithm to determine all eigenvalues up to a given energy for various configurations of the random potentials, i.e., for different samples. The samples had a size of 100×100 sites on a square lattice and $19 \times 19 \times 19$ sites on a simple cubic lattice; periodic boundary conditions were imposed. According to Eq. (2) we determine the density of states, which fluctuates strongly for a given sample. Averaging over 70 samples in two dimensions and 50 samples in three dimensions yields a sufficiently smooth density of states in the energy range around the Hartree band edge. To improve the statistics in the tails the average was taken over more and more samples at lower and lower energies. In the extreme tail we included 2100 samples and 350 samples for the Gaussian disorder case in two and three dimensions, respectively, and 700 samples for the binary disorder (two dimensions). Due to the comparatively large sample sizes, the data thus obtained are much more reliable than our previously published results of similar numerical simulations.¹⁷

VII. RESULTS

The above technique has been applied to a particle in a Gaussian-distributed disorder potential on a square and on a cubic lattice. The potential V has average zero and is delta correlated with a width $W = 1$ in the two-dimensional (2D) case and width $W = 4/3$ in three dimensions (3D). We have also solved numerically the nonlinear equation of motion (8) on a lattice of 13×13 and

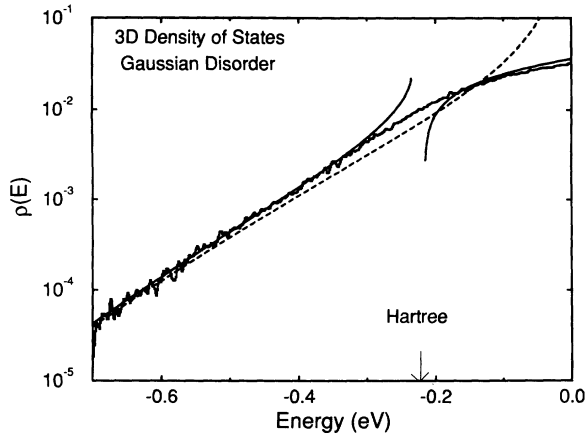


FIG. 1. Density of states (in eV^{-1}) for a tight-binding model on a cubic lattice in the presence of a random potential with Gaussian statistics. Histogram: data from the numerical simulation. Full curves: instanton after Hartree resummation (left part), Hartree summation inside the band (right part). Dashed curve: bare instanton theory. The effect of the resummation can be clearly seen. No fitting was done.

$9 \times 9 \times 9$ sites. The determinants were then calculated numerically. The results are presented in Figs. 1 and 2. In the absence of disorder, the unperturbed band edge lies at $E = 0$. In the presence of disorder there is a tail extending to $E = -\infty$. The dashed curve in Fig. (1) represents the predictions from the bare instanton calculation (12) and already gives a good description of the data for energies deep in the tail. The solid curves in the tail region (left part in the figures) are the predictions from the instanton theory after resummation, improving the theoretical prediction. The instanton with resummation

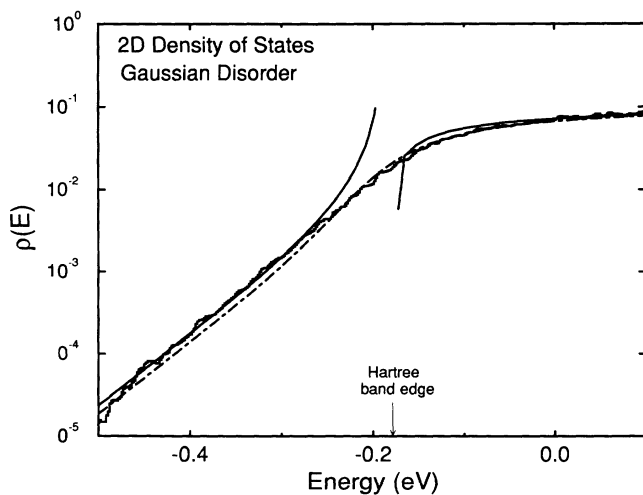


FIG. 2. Density of states (in eV^{-1}) for a tight-binding model on a square lattice in the presence of a random potential with Gaussian statistics. Histogram: data from the numerical simulation. Full curves: instanton after Hartree resummation (left part), Hartree summation inside the band (right part). Dotted-dashed line: CPA prediction. The CPA performs very well in the case of Gaussian disorder.

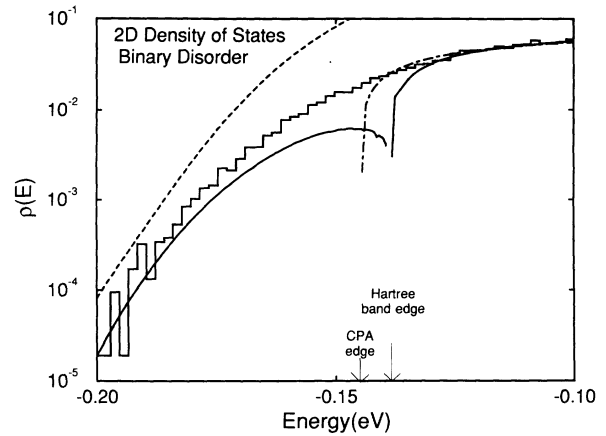


FIG. 3. Density of states (in eV^{-1}) for a tight-binding model on a square lattice with binary disorder. Histogram: data from the numerical simulation. Dashed curve: bare instanton theory. Full curves: instanton after Hartree resummation (left part), Hartree summation inside the band (right part). Dotted-dashed curve: CPA prediction, only present in the band.

coincides with the numerical data up to higher energies than does the bare instanton. The solid curves in the right part of the graphs are the results of our effective-medium theory. They were calculated with formulas (19) and (20) and agree very well with the numerical simulation.

We compared our results also to the CPA method as presented in Ref. 8. We recall that the self-energy in the CPA is calculated self-consistently:

$$\Sigma_{CPA}(E) = \int dV \nu(V) \frac{V}{1 - (V - \Sigma_{CPA})g_0(E - \Sigma_{CPA})}. \quad (24)$$

This self-energy is used to calculate the Green's function and the density of states. The CPA performs very well in the case of Gaussian disorder.⁸ This can be seen in Fig. 2, where the CPA is denoted by the dotted-dashed curve. For reasons of clearness we omitted the CPA in the three-dimensional case and the bare instanton in the two-dimensional case. The qualitative behavior in two and three dimensions is the same.

The same procedure was followed for a system with binary disorder distribution. The potential has zero mean and probability $\frac{1}{2}$ to be either $-1/\sqrt{12}$ or $1/\sqrt{12}$. The results are plotted in Fig. 3. The limited range of the CPA is evident (dotted-dashed line). The figure clearly shows a reasonable agreement between the numerical simulation and the bare instanton approach (dashed line). Again, resummation (solid line) improves the agreement.

VIII. SUMMARY

Both for Gaussian and for binary disorder and in both two and three dimensions we have obtained agreement between theory and simulations. It is important to note that the results are plotted without any fitting parame-

ters. All prefactors are explicitly taken into account in our theory. The predictions of our theory inside the band and in the tail describe almost the whole spectrum, except for a small “critical” region near the edge where our predictions diverge from the simulation experiment. It can also be seen that the Urbach rule, which would correspond to a straight line in our plots, works quite well in the Gaussian case, but not in the binary case.

In conclusion, we have presented a method to calculate the tail of the density of states of a disordered system. It includes all numerical prefactors and there are no adjustable parameters. It can be used in the continuum and on the lattice, in all dimensions. Arbitrary disorder distributions can be treated. The results of our method match the numerical data well, especially if the theory with resummation is used. We also presented an effective-medium theory to calculate the density of states

inside the band. This method also agrees with numerical simulation.

It may be possible to use the same technique to calculate transport properties like the ac conductivity of disordered systems. This calculation would be more elaborate as two-instanton solutions are needed.^{24,25}

ACKNOWLEDGMENTS

The idea of the effective-medium theory presented here is due to Roland Hayn, for which we are grateful. The authors would like to thank Jean-Marc Luck and Morell H. Cohen for discussions. The research of Th.M.N. was made possible by support from the Royal Netherlands Academy of Arts and Sciences (K.N.A.W.).

-
- ¹ M. H. Cohen, M. Y. Chou, E. N. Economou, S. John, and C. M. Soukoulis, *IBM J. Res. Dev.* **32**, 82 (1988).
² F. Urbach, *Phys. Rev.* **92**, 1324 (1953).
³ I. M. Lifshitz, *Adv. Phys.* **13**, 483 (1964).
⁴ B. I. Halperin, *Phys. Rev.* **139**, A104 (1965).
⁵ B. I. Halperin and M. Lax, *Phys. Rev.* **148**, 722 (1966).
⁶ P. Lloyd, *J. Phys. C* **2**, 1717 (1969).
⁷ P. van Mieghem, *Rev. Mod. Phys.* **64**, 755 (1992).
⁸ E. N. Economou, C. M. Soukoulis, M. H. Cohen, and A. D. Zdetsis, *Phys. Rev. B* **31**, 6172 (1985).
⁹ S. Abe and Y. Toyozawa, *J. Phys. Soc. Jpn.* **50**, 2185 (1981).
¹⁰ Q. Li, C. M. Soukoulis, and E. N. Economou, *Phys. Rev. B* **37**, 8289 (1988).
¹¹ S. John, M. Y. Chou, M. H. Cohen, and C. M. Soukoulis, *Phys. Rev. B* **37**, 6963 (1988).
¹² A. A. Klochikhin and S. G. Oglobin, *Phys. Rev. B* **48**, 3100 (1993).
¹³ J. L. Cardy, *J. Phys. C* **11**, L321 (1978).
¹⁴ E. Brézin and G. Parisi, *J. Phys. C* **13**, 307 (1980).
¹⁵ Th. M. Nieuwenhuizen, *Physica A* **167**, 43 (1990).
¹⁶ J. M. Luck and Th. M. Nieuwenhuizen, *J. Stat. Phys.* **52**, 1 (1988).
¹⁷ M. Schreiber and Y. Toyozawa, *J. Phys. Soc. Jpn.* **51**, 1528 (1982); **51**, 1537 (1982); **51**, 1544 (1982); **52**, 318 (1983).
¹⁸ M. C. W. van Rossum, Th. M. Nieuwenhuizen, E. Hofstetter, and M. Schreiber, in *Photonic Band Gaps and Localization*, Vol. 308 of *NATO Advanced Study Institute, Series B: Physics*, edited by C. M. Soukoulis (Plenum Press, New York, 1993).
¹⁹ K. N. Efetov, *Adv. Phys.* **32**, 53 (1983).
²⁰ Th. M. Nieuwenhuizen and J. M. Luck, *Europhys. Lett.* **9**, 407 (1989).
²¹ V. Glaser, S. Coleman, and A. Martin, *Commun. Math. Phys.* **58**, 211 (1978).
²² J. Zinn-Justin, *Quantum Field Theory and Critical Phenomena* (Clarendon, Oxford, 1989).
²³ Th. M. Nieuwenhuizen, *Phys. Rev. Lett.* **62**, 357 (1989).
²⁴ A. Houghton, L. Schäfer, and F. J. Wegner, *Phys. Rev. B* **22**, 3598 (1980).
²⁵ R. Hayn and W. John, *Nucl. Phys. B* **348**, 766 (1991).